ACS APPLIED MATERIALS & INTERFACES

Research Article

www.acsami.org

Flat-Lying Semiconductor–Insulator Interfacial Layer in DNTT Thin Films

Min-Cherl Jung,[†,‡] Matthew R. Leyden,[†,‡] Gueorgui O. Nikiforov,[†] Michael V. Lee,[†] Han-Koo Lee,[§] Tae Joo Shin,[§] Kazuo Takimiya,[⊥] and Yabing Qi*[,†]

[†]Energy Materials and Surface Sciences Unit (EMSS), Okinawa Institute of Science and Technology Graduate University (OIST), 1919-1 Tancha, Onna-son, Okinawa 904-0495, Japan

[§]Pohang Accelerator Laboratory, POSTECH, Pohang 790-784, Republic of Korea

[⊥]Emergent Molecular Function Research Group, RIKEN Center for Emergent Matter Science (CEMS), 2-1 Hirosawa, Wako, Saitama 351-0198, Japan

Supporting Information

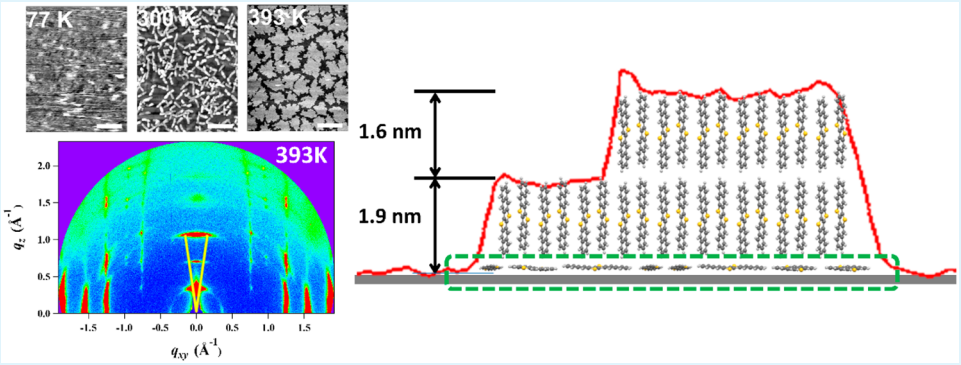

ABSTRACT: The molecular order of organic semiconductors at the gate dielectric is the most critical factor determining carrier mobility in thin film transistors since the conducting channel forms at the dielectric interface. Despite its fundamental importance, this semiconductor–insulator interface is not well understood, primarily because it is buried within the device. We fabricated dinaphtho[2,3-*b*:2′,3′-*f*]thieno[3,2-*b*]thiophene (DNTT) thin film transistors by thermal evaporation in vacuum onto substrates held at different temperatures and systematically correlated the extracted charge mobility to the crystal grain size and crystal orientation. As a result, we identify a molecular layer of flat-lying DNTT molecules at the semiconductor–insulator interface. It is likely that such a layer might form in other material systems as well, and could be one of the factors reducing charge transport. Controlling this interfacial flat-lying layer may raise the ultimate possible device performance for thin film devices.

KEYWORDS: *DNTT, vacuum evaporation, GIXD, NEXAFS, AFM*

1. INTRODUCTION

When the gate of a field-effect transistor is biased, the electric field forms a conducting channel at the dielectric interface. The molecular order of organic semiconductors in the channel at this interface is the most critical factor determining carrier mobility in thin film transistors (TFTs).[1−3] Charge mobility, as extracted from transistor $I-V$ measurements, varies not only with the semiconductor, but also with the combination of the dielectric with the semiconductor.[1−3] The gate dielectric can influence charge mobility through physical or electronic interactions. For instance, a high surface energy surface will interact more strongly with polar or polarizable faces of crystals. Rough surfaces more readily initiate crystal growth and would be expected to produce multicrystalline films with smaller grains and a broader distribution of crystal orientations. Random dipoles at the surface, as measured by permittivity, which may be produced by the chemical termination of the dielectric surface or by defects near the surface of the dielectric, tend to produce charge traps or dope an organic semiconductor film on top of it.[4] This effect is observed even when the gate dielectric is physically laminated onto separately grown high-quality single crystals[5] or when the gate dielectric is a polar gas vs vacuum.[6] To alleviate these issues, various techniques, such as monolayer modifications, introduction of intermediate layers, or post-treatments, have been devised.[7,8]

Despite its fundamental importance, the nature of the semiconductor–insulator interface is not well understood primarily because it is buried within the device. Often the

Received: October 30, 2014
Accepted: December 29, 2014
Published: December 29, 2014

DOI: 10.1021/am507528e
ACS Appl. Mater. Interfaces 2015, 7, 1833−1840

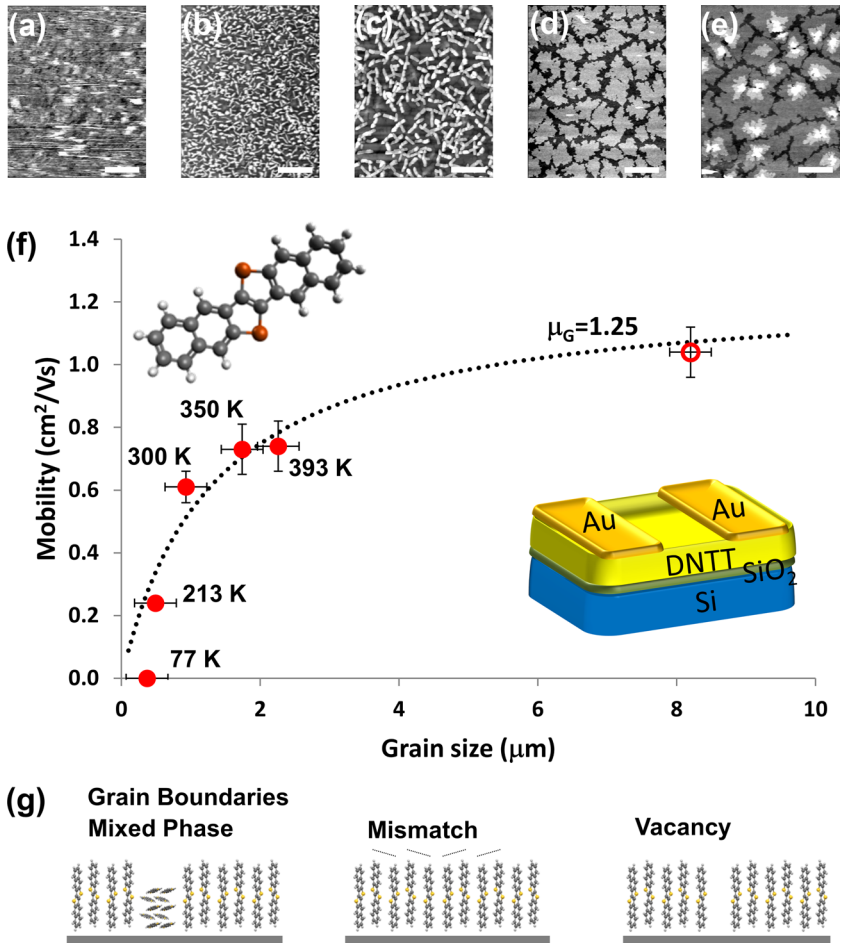

Figure 1. Relationship between grain size and field-effect mobility. (a–e) Atomic force microscope height images with increasing grain sizes. The white scale bar is 2 μm in each image. (a) 77 K the molecules were not able to diffuse and the film is irregular. (b) 213 K and (c) 298 K combination of planar phase with distinct grains and rod phase DNTT growing on top. (d) 350 K and (e) 393 K thin films have distinct grains larger than in films formed at lower temperatures. (f) Graph of field-effect mobility versus grain size. Insets show the molecular structure of DNTT and the structure of the transistor devices. Filled circles were fitted using the model in the paper. Open circle was not included for fitting but used to confirm the model and fit. (g) Possible boundaries between grains. In the central pane, the dotted lines are guides for the eye to show the crystal mismatch.

interface is complicated by additional monolayers. Organic semiconducting acenes or thienothiophenes are also typically modified with alkyl functional groups. With either monolayers on the dielectric or alkyl functional groups on the semiconductor, an additional alkyl layer is inserted into the interface. Here, we avoided this confounding effect by using dinaphtho[2,3-*b*:2′,3′-*f*]thieno[3,2-*b*]thiophene (DNTT), one of the most studied and highest mobility thienothiophenes that is free of additional alkyl chains. Thienothiophenes have higher stability against oxidation than acenes like pentacene. We report findings on thermally evaporated DNTT films deposited directly on native silicon dioxide substrates at temperatures between 77 to 400 K. This combination of DNTT directly on silicon dioxide provides one of the simplest interfaces possible for a field-effect device. We identify a molecular layer of flat-lying DNTT molecules at the semiconductor–insulator interface, which could be one of the factors affecting charge transport and ultimately device performance.

2. EXPERIMETAL PROCEDURES

2.1. Fabrication Methods. Most DNTT thin films in this study were deposited at a fixed rate of 0.6 Å/s on silicon dioxide substrates that were held at temperatures between 400 to 77 K. The samples with the largest grains were fabricated at a low rate of 0.1 Å/min deposited on a substrate at room temperature.

2.2. Transistor Measurement Methods and Mobility Determination. The output and transfer characteristics of the DNTT thin film transistors were measured in ambient air using a Keithley 4200 SPA. The voltages that were applied to the source-drain and gate were in the range of $-60\ \text{V} \le V_{ds} \le 0\ \text{V}$ and $-60\ \text{V} \le V_g \le 0\ \text{V}$. Channel lengths were 100 μm and widths were 2 mm or 3 mm. Both the forward and reverse scans were recorded in order to detect any hysteresis. In most cases the devices exhibited very good characteristics with a well-defined saturation regime, low contact resistance, low leakage current of 1×10^{-10} A (factor of 1×10^6 lower than the on-current of the transistor in saturation regime) and ON/OFF ratio on the order of 1×10^5. The charge mobility μ of the DNTT thin film transistors in this study was extracted from their transfer characteristics using the following two formulas

$$I_{d(lin)} = \mu_{lin} C_g \frac{W}{L}(V_g - V_t)V_{ds} \quad (1)$$

$$I_{d(sat)} = \frac{1}{2}\mu_{sat} C_g \frac{W}{L}(V_g - V_t)^2 \quad (2)$$

Where the subscripts lin and sat refer to the linear and saturation regimes, respectively; I_d is the drain current, C_g is the gate dielectric capacitance per unit area; V_g, V_t, and V_{ds} are the gate, threshold, and source-drain voltages; and W and L are the channel width and length, respectively. The mobility values as a function of temperature, shown in

DOI: 10.1021/am507528e
ACS Appl. Mater. Interfaces 2015, 7, 1833–1840

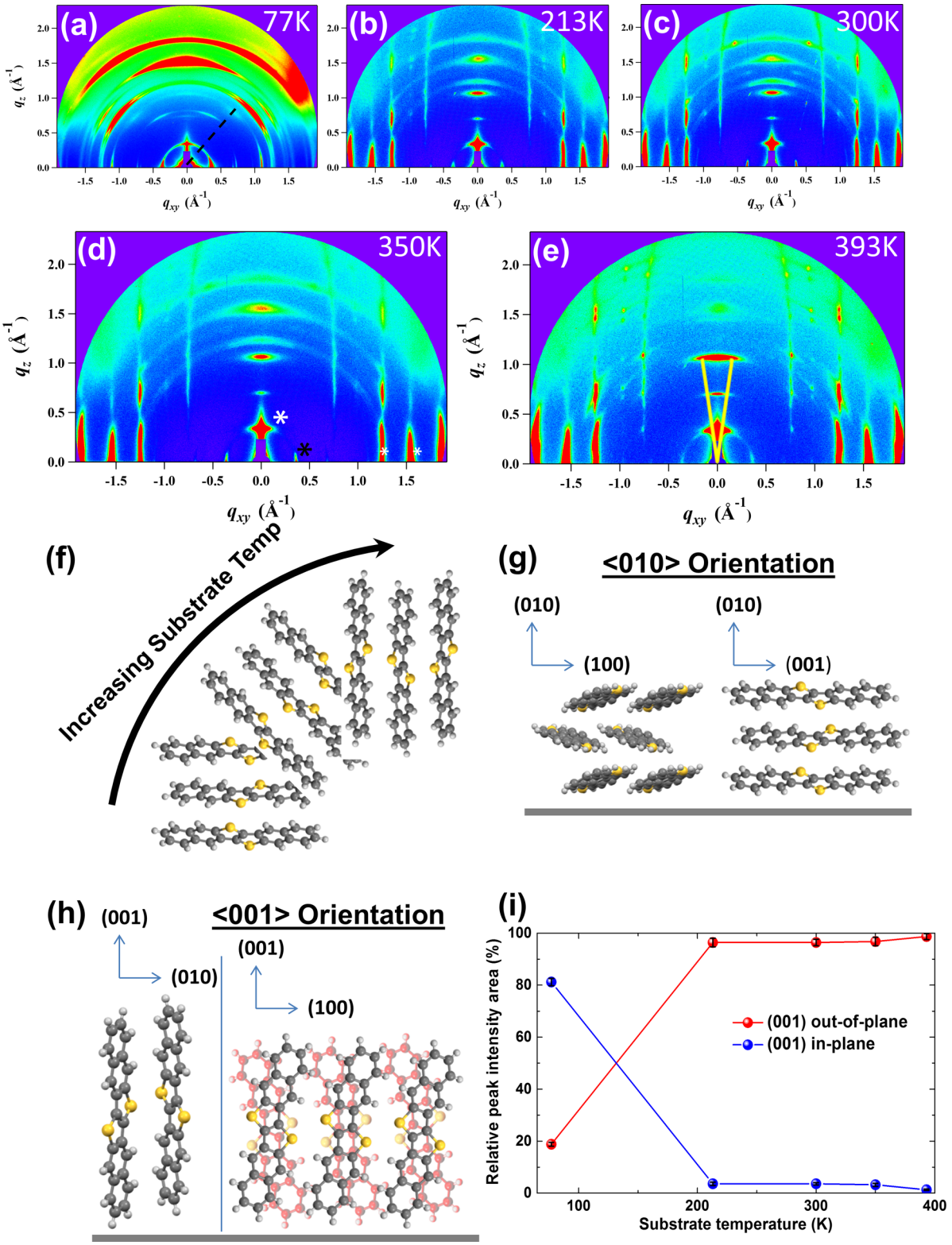

Figure 2. 3D GIXD cross-sections from samples prepared at (a) 77, (b) 213, (c) 300, (d) 350, and (e) 393 K. Black dashed line in a identifies the off-axis (003) peak. The yellow lines in e highlight the variation in orientation in the sample prepared at 393 K. (f) Above 200 K, ⟨001⟩ orientation is dominant. (g) ⟨010⟩ orientation represented by the in-plane (001) peak. (h) ⟨001⟩ orientation represented by the out-of-plane (001) peak. (i) Relative intensity of each orientation.

Figure 1f represent the saturation mobility μ_{sat} extracted from transfer curves measured at $V_{ds} = -60$ V. Representative curves from each device are presented in Figure S1 in the Supporting Information.

2.3. Grazing Incidence X-ray Diffraction Measurements. Grazing-incidence X-ray diffraction (GIXD) measurements were conducted at PLS-II 9A U-SAXS beamline of Pohang Accelerator Laboratory in Korea. The X-rays coming from the in-vacuum undulator (IVU) are monochromated (wavelength λ = 1.109 Å) using a double crystal monochromator and focused both horizontally and vertically (450 (H) x 60 (V) μm^2 in fwhm @ sample position) using K−B type

DOI: 10.1021/am507528e
ACS Appl. Mater. Interfaces 2015, 7, 1833−1840

Table 1. Crystallographic Parameters Derived from GIXD Analysis

crystallographic parameters		77 K	213 K	300 K	350 K	393 K
(001) peak from q_z profile	q (Å^{-1})	0.3837	0.3831	0.3831	0.3855	0.3848
	d-spacing (Å)	16.4	16.4	16.4	16.3	16.3
	fwhm (Å^{-1})	0.02420	0.02404	0.02420	0.02054	0.02244
	⟨001⟩ abundance	18.8%	94.4%	96.4%	96.8%	98.7%

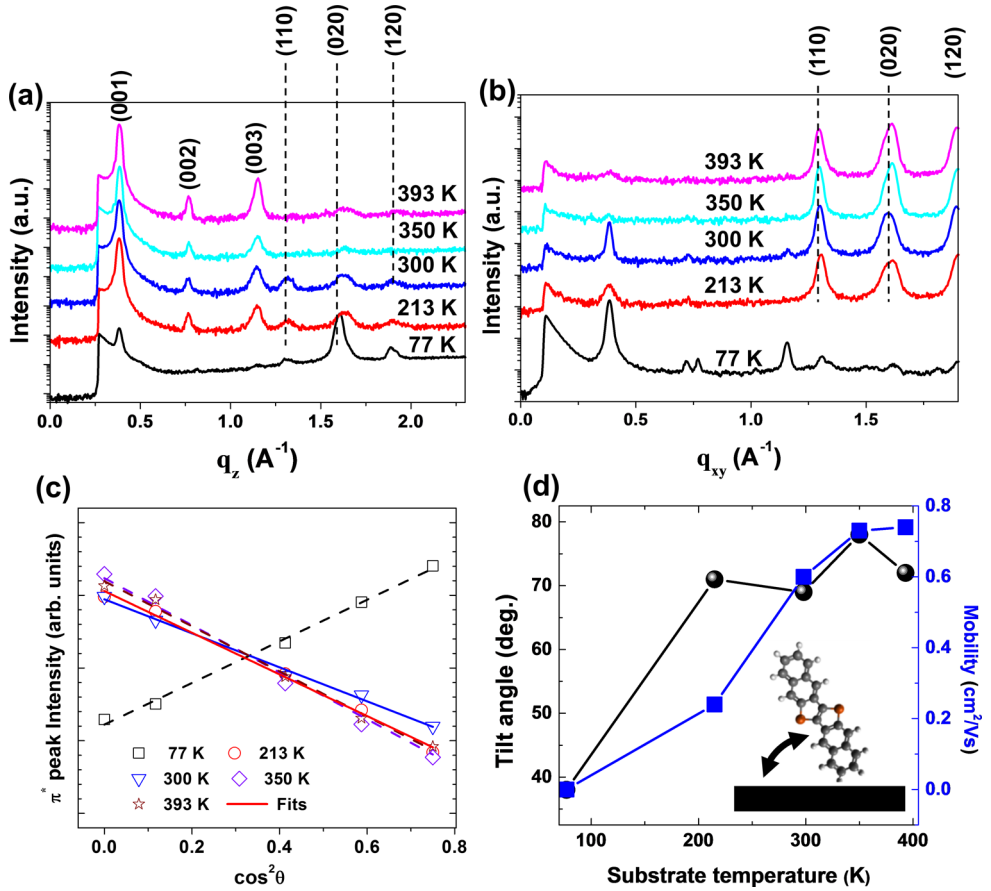

Figure 3. (a) Out-of-plane (q_z) and (b) in-plane (q_{xy}) diffraction profiles extracted from GIXD images of Figure 2a–e. The ⟨001⟩ orientation and ⟨010⟩ orientation is designated when (00l) peaks or (0k0) peaks appear only in the out-of-plane GIXD profile, respectively. (c) Measurement of π^* peak intensity relative to incident angle from angle-resolved NEXAFS for calculating molecular tilt angle. (d) Molecular tilt angle calculated from the angle dependent π^* peak intensity and corresponding field-effect mobility prepared at 77, 213, 300, 350, and 393 K.

mirrors. The GIXD sample stage is equipped with a 7-axis motorized stage for the fine alignment of sample and the incidence angle of the X-ray beam was set in the range of 0.1–0.15°, which is close to the critical angle of DNTT. GIXD patterns were recorded with a 2D CCD detector (Rayonix SX165) and X-ray irradiation time was 2–40 s dependent on the saturation level of detector. Diffraction angles were calibrated by a precalibrated sucrose (Monoclinic, P21, a = 10.8631 Å, b = 8.7044 Å, c = 7.7624 Å, b = 102.938°)[9] and the sample-to-detector distance was about 225.5 mm.

2.4. Measurements of Near-Edge X-ray Absorption of Fine Structure. All the NEXAFS measurements were performed at room temperature at the 2A elliptically polarized undulator (EPU) beamline of the Pohang Light Source (PLS). We used the partial-electron-yield detection mode for NEXAFS spectra by recording the sample current normalized to a signal current measured simultaneously using a gold mesh in ultrahigh vacuum. We used a polarized (p-polarized) synchrotron photon beam (~100%) with an energy in the range of 279–320 eV with a spectral energy resolution of ΔE = 100 meV and a probing depth of ~20 Å for surface-sensitive measurements.

3. RESULTS AND DISCUSSION

The DNTT films form as expected and are similar to those prepared with pentacene by other groups. We observed 4 different morphologies on films with a thickness of ~20–30 nm: amorphous, rod, planar, and bulk (Figure 1a–e), which are consistent with pentacene films.[10−13] In AFM, the films deposited at 77 K appear amorphous and of low density (Figure 1a).

At deposition temperatures above 77 K, planar grains form and merge into a planar film (Figure 1b–e). At intermediate temperatures the rod morphology forms atop films thicker than a few monolayers, and appears as tall, narrow features. At higher temperatures, we see bulk phase formation.[13] The similarity between the above findings on DNTT and previous reports on pentacene is not surprising because of the similar molecular structures of the two materials. Film thicknesses of 30 nm were used in most cases in this work, but the grain sizes of the films prepared at 350 and 400 K were difficult to discern, so films were also prepared at these temperatures with only 2–5

DOI: 10.1021/am507528e
ACS Appl. Mater. Interfaces 2015, 7, 1833–1840

monolayers so that the grain sizes could be accurately measured. The sizes of the crystal grains in the planar region in samples deposited at 213, 300, 350, and 393 K were 0.5, 0.9, 1.7, and 2.3 μm, respectively. The sample deposited at 77 K did not show a clear planar phase, and instead we put an upper bound of 0.3 μm based on the apparent size of grains.

The electronic properties of field-effect devices using our DNTT films are similar to those found in the literature. The mobility values extracted from the saturation regime of I−V measurements on transistors comprising those films, are plotted against grain size in Figure 1(f). The transistor mobility increases as a function of substrate temperature for the same evaporation rate, which could be attributed to the larger crystal grain sizes and fewer grain boundaries in films deposited at higher temperatures. The films prepared at 77 K, which do not contain a planar phase, exhibited very poor transistor performance having a mobility of $\sim 2 \times 10^{-4}$ cm^2 V^{-1} s^{-1}. At higher temperatures of 213, 300, 350, and 393 K the respective extracted mobility values were 0.24 ± 0.02, 0.61 ± 0.05, 0.73 ± 0.08, and 0.74 ± 0.09 cm^2 V^{-1} s^{-1}. These values are consistent with previous reports on the mobility of DNTT films grown on silicon dioxide.[14,15]

The relationship between grain size and mobility can be fitted reasonably well using a theory, developed for other organic semiconductor systems, that treats grain boundaries as an energy potential barrier.[16,17] The nature of the grain boundaries is unknown, but could be composed of an air gap, different crystal phases, or crystal mismatch between the grains, as depicted in Figure 1g. The grain boundaries in DNTT films are likely similar to those in pentacene films. The effective mobility, μ_{eff} is expressed as

$$\mu_{\text{eff}} = \frac{\mu_{\text{G}}}{1 + \alpha \frac{\mu_{\text{G}}}{L_{\text{G}}} e^{qV_{\text{b}}/kT}} \tag{3}$$

where μ_{G} is the charge mobility within a single grain, L_{G} is the grain size, and α is the hopping or tunneling probability across boundaries or the probability for a charge to hop vertically to the next crystal layer, which might also form a connecting channel between grains.[18] V_{b} is the height of the potential barrier at the grain boundaries. The best fit to the data (Figure 1f) is obtained for $\mu_{\text{G}} = 1.25$ cm^2 V^{-1} s^{-1}. The data point in Figure 1f with a grain size of 8.2 μm is from a DNTT film deposited at a very low rate at room temperature. The corresponding mobility value is 1.04 cm^2 V^{-1} s^{-1}. This is the highest mobility to-date for DNTT thin films deposited directly on silicon dioxide and fits eq 3 very well. Therefore, to the extent to which the simplifying assumptions behind eq 3 are valid, the charge mobility within a single grain of our prepared films on silicon dioxide is 1.25 cm^2 V^{-1} s^{-1}. This value is consistent with the literature, is lower than the measured mobility of ~10 cm^2 V^{-1} s^{-1} for an ideal interface of transistor with a vacuum gap on single crystal,[19] and is lower than a mobility value between 2.5 and 4 cm^2 V^{-1} s^{-1} measuared for single-crystal DNTT transistors using a fluorinated CYTOP dielectric.[20] The nature of the interface between the dielectric and organic semiconductor reduces the mobility of the films relative to the single-crystal mobility with an ideal dielectric or a nonpolar, low surface free energy dielectric.[4]

The films are multicrystalline and principally composed of grains with the preferred DNTT orientation. We performed multidimensional synchrotron GIXD experiments in order to study the crystallinity of the prepared thin films and understand the film structure (Figure 2a−e, Table 1). The GIXD data fit well to the monoclinic space group $P2_1$ characteristic for DNTT crystals indicating that the structure of our polycrystalline thin films is the same as that for single crystals (Figure 3a, b, and Figure S2 in the Supporting Information).[14] According to theory, for crystal grains with a ⟨001⟩ orientation, the (00l) peaks appear in the out-of-plane (q_z) direction, whereas the (110), (020), and (120) peaks appear in the in-plane (q_{xy}) direction. In contrast, for crystal grains with a ⟨010⟩ orientation, the (00*l*) peaks appear in the q_{xy} direction, and the (020) peak appears in the q_z direction. On the basis of that argument and given our GIXD data, only two crystal orientations are present in each of the films: the preferred ⟨001⟩ crystal orientation (Figure 2h), which is dominant in all the films prepared above 200 K (Figure 2d, white stars) and is considered to give the best transistor characteristics; and the ⟨010⟩ orientation (Figure 2g), which is dominant in the films prepared at 77 K (Figure 2a), and is also present in trace amounts in the other films (Figure 2d, black stars). Higher substrate temperatures increase the relative proportion of the ⟨001⟩ orientation and reduce the relative proportion of the ⟨010⟩ orientation. It is interesting to note that based on the GIXD data, the rod morphology shown in Figure 1b, c shares the same crystal structure as the planar morphology (Figure 1d, e). Furthermore, there are two exceptions to the pure ⟨010⟩ or ⟨001⟩ orientations for the crystalline molecules. In Figure 2e the (*00l*) peaks form an arc, which is about 5° wider than is observed for the samples prepared at other temperatures, indicating that in that case grains are beginning to deviate from the ⟨001⟩ orientation.[21] This deviation is consistent with a transition from planar to bulk phase growth of the DNTT films. There is also an additional weak (001) peak at 40° from the surface normal in the GIXD for the 77 K sample.

The relative abundance of the two main crystal orientations can be calculated by integrating the intensity of the (001) peak and comparing the relative integrated intensity in-plane and out-of-plane. The relative integrated areas for each crystal orientation were calculated and plotted in Figure 2i, taking into account the broad peak in Figure 2e. The values for the ⟨001⟩ orientation are listed in Table 1. Pole figures are not necessary because there are only two crystal structures observed in most of the samples. The exception is the 77 K sample, which has an additional peak. However, for this analysis the additional (001) peak observed in the 77 K sample was ignored, so the relative abundance of ⟨001⟩ orientation may be underestimated.

The films also include a minor component of DNTT molecules that are oriented with the molecular plane parallel to the dielectric surface. The GIXD data indicates that for films, deposited at temperatures above 200 K, the preferred molecular orientation is ⟨001⟩, where the molecular long axis is oriented approximately orthogonal to the substrate. Therefore, judging from the GIXD data alone, one would expect that on average, all molecules are oriented in the ⟨001⟩ direction. However, the tilt of the plane of the DNTT molecules is about 85° relative to the ⟨001⟩ direction.[14] GIXD detects only crystalline regions of the film and this data needs to be complemented by spectroscopic measurements that do not depend on crystallinity. According to NEXAFS, which does not depend on crystallinity, the average molecular orientation is 70−80° instead of 85° (Figure 3c, d). If we assume that the minor components of the film are composed of randomly oriented molecules (magic angle 55°), then 7−34% of the film would need to be randomly oriented to bring the average molecular orientation down to 70−80°. Such a high proportion of randomly oriented molecules would be readily observable in surface scans by AFM and also obvious as a background in the GIXD data. Neither of these was observed. On

DOI: 10.1021/am507528e
ACS Appl. Mater. Interfaces 2015, 7, 1833−1840

the other hand, if we assume that the minor components of the film are composed of molecules lying flat then only 2−11% of the film would need to be prostrate on the surface for the average molecular orientation to be 70−80°. Therefore, it can be concluded that the reason why the result of the NEXAFS measurement is 70−80° as opposed to 85° is that, whereas the majority of the film is crystalline with the molecules standing up, a small percentage of the film is prostrate on the surface. At least half of the prostrate molecules can be explained by the minor crystalline component. The rest would be amorphous.

A thin interfacial flat-lying layer of DNTT between the DNTT films and the silicon dioxide dielectric surface helps account for the angle. On the basis of the data and analysis so far, we have shown that thin films of DNTT thermally evaporated on silicon dioxide are predominantly crystalline with the molecules oriented orthogonally to the sample surface and have a small component composed of molecules lying flat. It is not clear exactly how this flat-lying component is scattered throughout the film, however considering that for TFT applications, the most important part of the film is the interfacial layer with the insulator, it is worth examining more closely with AFM on ultrathin DNTT films composed of only a couple of monolayers. Such a representative scan is shown in Figure 4a, where 1−2 monolayers are deposited at a substrate temperature of ∼400 K. A histogram of the heights in Figure 4a is shown in Figure 4b. The height of the first layer is 1.90 ± 0.14 nm and the height of the second layer is 1.64 ± 0.15. Further details can be found in the Supporting Information. A single layer of crystalline DNTT is 1.62 nm,[14] whereas the added height of the first layer is roughly the thickness of one DNTT molecule. We reviewed all of our images on samples at early stages of growth, using both contact mode and AC mode, and found that in all instances the bottom layer was consistently thicker than subsequent layers by roughly the same amount. No difference was observed in phase contrast that would indicate that this is an artifact. Our height scale was confirmed by imaging Au(111) atomic steps on a freshly annealed Au (150 nm)/mica sample; the measured step height from multiple images was 0.23 ± 0.01 nm. Thus, we conclude that there is an intermediate layer of flat-lying DNTT that forms at the interface between the substrate and the crystalline DNTT film in all of our samples.

The interfacial layer may be related to the growth mechanism for evaporated films. Planar polyaromatic molecules initially deposit on a substrate most likely in the flat-lying geometry, and diffuse to a growing crystal grain where they upright themselves to match the crystal lattice to lower their free energy. At 77 K, the molecules would not reorient themselves very easily during the growth process. Some of these molecules could remain in the flat-lying configuration even with higher substrate temperature during deposition while the crystalline grains grow over them. A layer of DNTT molecules would present a reduced energy surface and lower the energy barrier for subsequent molecules to be oriented orthogonal to the substrate—modifying the surface energy essentially the same way as a self-assembled monolayer would do. This phenomenon would not be limited to DNTT on silicon dioxide, and might be expected with any organic semiconductor grown on a surface with a high surface free energy. Such an interfacial layer would be consistent with the observations in the literature of pentacene thin films by X-ray reflectivity measurements and surface enhanced Raman scattering.[22,23] Indeed, based on spectroscopic evidence alone, a similar interfacial layer was suggested to form when pentacene is deposited on a metal surface.[24]

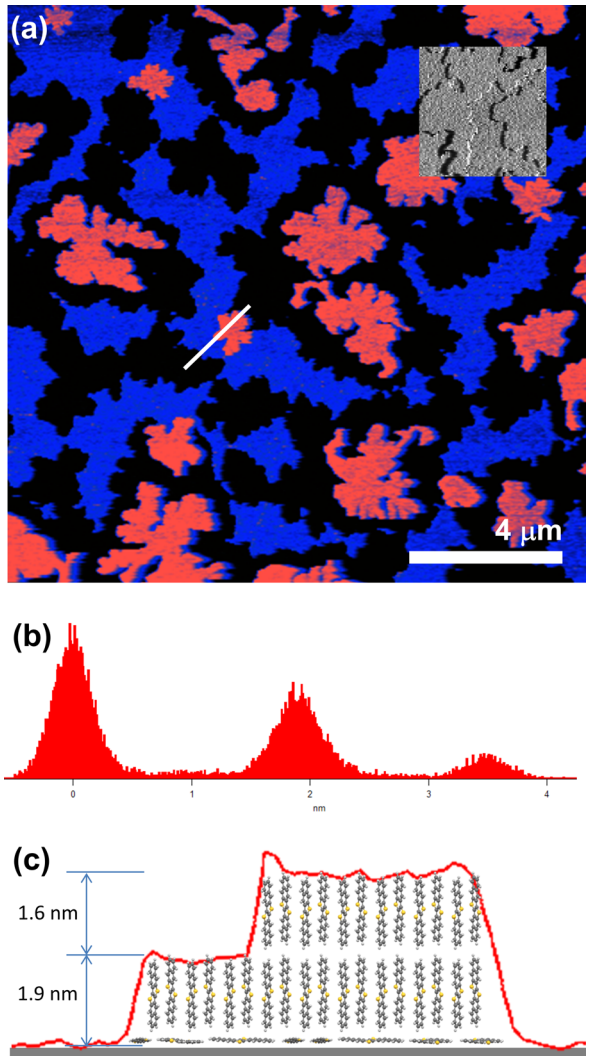

Figure 4. AFM height analysis. (a) AFM image of 1−2 monolayer film in tapping mode. Blue color (first layer) is 1.9 nm above the surface. Salmon color (second layer) is 1.6 nm taller than the first layer. Scale bar is 4 μm. Inset grayscale box shows phase information for a region including substrate, first layer, and second layer. (b) Histogram of a subset of the entire image. (c) Line scan from a including scaled images of DNTT molecule representing a possible structure for the film.

An interfacial layer right at the dielectric surface could have dramatic implications. Although it is established that charge transport in organic TFTs occurs close to the semiconductor−insulator interface, the thickness of the channel is still being debated. Some theoretical models treat the charge area as a 2D gas,[25,26] whereas others as a 3D distribution[27] and both of these models fit experimental data quite well. Furthermore, several reports on pentacene claim that anywhere between 2 and 6 monolayers, or about 3−9 nm, are involved in the transport.[28−30] Although different estimates vary, the thickness of the channel is clearly very small and the electric field in the channel would be highest adjacent to the dielectric, which suggests that the interfacial layer that we have identified certainly plays an important role. At the surface of the dielectric, it would feel the electric field stronger than the rest of the channel when the gate is biased. This layer could act as a source of hole traps or local differences in dipoles that degrade organic device performance.[31] It might also influence subsequent crystal growth, leading to more mismatch or defects within grains. On the other hand,

DOI: 10.1021/am507528e
ACS Appl. Mater. Interfaces 2015, 7, 1833−1840

lowering the surface free energy of silicon dioxide by this intermediate layer might be required for the preferred crystal orientation to form on a dielectric without a self-assembled monolayer. As a whole, although further studies are warranted, it is already clear that this single monolayer of molecules could have dramatic implications for organic semiconductor crystal growth and properties of organic semiconductor devices grown on oxides.

4. CONCLUSION

On the basis of GIXD and AFM studies, we conclude that DNTT films are polycrystalline, consistent with previously reported results in the literature, and are principally composed of ⟨001⟩ orientation. The films also include some portion with ⟨010⟩ orientation that is usually minor, but dependent on film formation temperature. On the basis of statistical analysis of AFM images showing a 1.9 nm thick first layer, and the requirement of only upright or prostrate molecules in the film, we conclude that an interfacial flat-lying layer of DNTT molecules forms between the preferred orientation DNTT film and the dielectric surface. This interfacial layer exists in the region with the highest electric field of the device channel of a field-effect transistor, and as such could have significant implications for device performance.

■ ASSOCIATED CONTENT

Ⓢ Supporting Information

Output curves, transfer curves, and curves for extracting μ from representative devices prepared at each temperature. Details about the equation relating mobility to grain size. Comparison between experimental data and single-crystal peaks. NEXAFS spectra. Details about statistical analysis of AFM images. This material is available free of charge via the Internet at http://pubs.acs.org.

■ AUTHOR INFORMATION

Corresponding Author

*E-mail: Yabing.Qi@oist.jp. Tel: +81-998-966-8435.

Author Contributions

‡M.-C.J. and M.L contributed equally.The manuscript was written through contributions of all authors. All authors have given approval to the final version of the manuscript.

Funding

Y.B.Q. acknowledges the financial support from Okinawa Institute of Science and Technology Graduate University.

Notes

The authors declare no competing financial interest.

■ ABBREVIATIONS

DNTT, dinaphtho[2,3-*b*:2′,3′-*f*]thieno[3,2-*b*]thiophene
OFET, organic field-effect transistor
GIXD, grazing incidence X-ray diffraction
NEXAFS, near-edge X-ray absorption of fine structure
AFM, atomic force microscopy

■ REFERENCES

(1) Nicolai, H. T.; Kuik, M.; Wetzelaer, G. a. H.; de Boer, B.; Campbell, C.; Risko, C.; Brédas, J. L.; Blom, P. W. M. Unification of Trap-Limited Electron Transport in Semiconducting Polymers. *Nat. Mater.* **2012**, *11*, 882−887.
(2) Qu, M.; Li, H.; Liu, R.; Zhang, S.-L.; Qiu, Z.-J. Interaction of Bipolaron with the H_2O/O_2 Redox Couple Causes Current Hysteresis in Organic Thin-Film Transistors. *Nat. Commun.* **2014**, *5*, 3185.
(3) Veres, J.; Ogier, S.; Lloyd, G.; de Leeuw, D. Gate Insulators in Organic Field-Effect Transistors. *Chem. Mater.* **2004**, *16*, 4543−4555.
(4) Veres, J.; Ogier, S. d.; Leeming, S. w.; Cupertino, D. c.; Mohialdin Khaffaf, S. Low-K Insulators as the Choice of Dielectrics in Organic Field-Effect Transistors. *Adv. Funct. Mater.* **2003**, *13*, 199−204.
(5) Yi, H. T.; Chen, Y.; Czelen, K.; Podzorov, V. Vacuum Lamination Approach to Fabrication of High-Performance Single-Crystal Organic Field-Effect Transistors. *Adv. Mater.* **2011**, *23*, 5807−5811.
(6) Chen, Y.; Podzorov, V. Bias Stress Effect in "Air-Gap" Organic Field-Effect Transistors. *Adv. Mater.* **2012**, *24*, 2679−2684.
(7) Kim, C.; Facchetti, A.; Marks, T. J. Polymer Gate Dielectric Surface Viscoelasticity Modulates Pentacene Transistor Performance. *Science* **2007**, *318*, 76−80.
(8) Liu, C.; Minari, T.; Li, Y.; Kumatani, A.; Lee, M. V.; Pan, S. H. A.; Takimiya, K.; Tsukagoshi, K. Direct Formation of Organic Semiconducting Single Crystals by Solvent Vapor Annealing on a Polymer Base Film. *J. Mater. Chem.* **2012**, *22*, 8462−8469.
(9) Hynes, R. C.; Le Page, Y. Sucrose, a Convenient Test Crystal for Absolute Structures. *J. Appl. Crystallogr.* **1991**, *24*, 352−354.
(10) Ruiz, R.; Choudhary, D.; Nickel, B.; Toccoli, T.; Chang, K.-C.; Mayer, A. C.; Clancy, P.; Blakely, J. M.; Headrick, R. L.; Iannotta, S.; Malliaras, G. G. Pentacene Thin Film Growth. *Chem. Mater.* **2004**, *16*, 4497−4508.
(11) Yanagisawa, H.; Tamaki, T.; Nakamura, M.; Kudo, K. Structural and Electrical Characterization of Pentacene Films on SiO_2 Grown by Molecular Beam Deposition. *Thin Solid Films* **2004**, *464*−*465*, 398−402.
(12) Tao, C.; Liu, Q.; Riddick, B. C.; Cullen, W. G.; Reutt-Robey, J.; Weeks, J. D.; Williams, E. D. Dynamic Interfaces in an Organic Thin Film. *Proc. Natl. Acad. Sci. U. S. A.* **2008**, *105*, 16418−16425.
(13) Bouchoms, I. P. M.; Schoonveld, W. A.; Vrijmoeth, J.; Klapwijk, T. M. Morphology Identification of the Thin Film Phases of Vacuum Evaporated Pentacene on SiO_2 Substrates. *Synth. Met.* **1999**, *104*, 175−178.
(14) Yamamoto, T.; Takimiya, K. Facile Synthesis of Highly π-Extended Heteroarenes, Dinaphtho[2,3-b:2‘,3‘-f]chalcogenopheno[3,2-B]chalcogenophenes, and Their Application to Field-Effect Transistors. *J. Am. Chem. Soc.* **2007**, *129*, 2224−2225.
(15) Kang, M. J.; Doi, I.; Mori, H.; Miyazaki, E.; Takimiya, K.; Ikeda, M.; Kuwabara, H. Alkylated Dinaphtho[2,3-b:2′,3′-f]Thieno[3,2-b]-Thiophenes (Cn-DNTTs): Organic Semiconductors for High-Performance Thin-Film Transistors. *Adv. Mater.* **2011**, *23*, 1222−1225.
(16) Hu, Y.; Qi, Q.; Jiang, C. Influence of Different Dielectrics on the First Layer Grain Sizes and Its Effect on the Mobility of Pentacene-Based Thin-Film Transistors. *Appl. Phys. Lett.* **2010**, *96*, 133311.
(17) Carlo, A. D.; Piacenza, F.; Bolognesi, A.; Stadlober, B.; Maresch, H. Influence of Grain Sizes on the Mobility of Organic Thin-Film Transistors. *Appl. Phys. Lett.* **2005**, *86*, 263501.
(18) Yang, H.; Shin, T. J.; Ling, M.-M.; Cho, K.; Ryu, C. Y.; Bao, Z. Conducting AFM and 2D GIXD Studies on Pentacene Thin Films. *J. Am. Chem. Soc.* **2005**, *127*, 11542−11543.
(19) Xie, W.; Willa, K.; Wu, Y.; Häusermann, R.; Takimiya, K.; Batlogg, B.; Frisbie, C. D. Temperature-Independent Transport in High-Mobility Dinaphtho-Thieno-Thiophene (DNTT) Single Crystal Transistors. *Adv. Mater.* **2013**, *25*, 3478−3484.
(20) Uno, M.; Tominari, Y.; Yamagishi, M.; Doi, I.; Miyazaki, E.; Takimiya, K.; Takeya, J. Moderately Anisotropic Field-Effect Mobility in dinaphtho[2,3-b:2′,3′-f]thiopheno[3,2-B]thiophenes Single-Crystal Transistors. *Appl. Phys. Lett.* **2009**, *94*, 223308.
(21) DeLongchamp, D. M.; Kline, R. J.; Fischer, D. A.; Richter, L. J.; Toney, M. F. Molecular Characterization of Organic Electronic Films. *Adv. Mater.* **2011**, *23*, 319−337.
(22) Woll, A. R.; Desai, T. V.; Engstrom, J. R. Quantitative Modeling of in Situ X-Ray Reflectivity during Organic Molecule Thin Film Growth. *Phys. Rev. B* **2011**, *84*, 075479.

DOI: 10.1021/am507528e
ACS Appl. Mater. Interfaces 2015, 7, 1833−1840

(23) Xu, J.; Diao, Y.; Zhou, D.; Mao, Y.; Giri, G.; Chen, W.; Liu, N.; Mannsfield, S. C. B.; Xue, G.; Bao, Z. Probing the Interfacial Molecular Packing in TIPS-Pentacene Organic Semiconductors by Surface Enhanced Raman Scattering. *J. Mater. Chem. C* **2014**, *2*, 2985−2991.
(24) Lukas, S.; Söhnchen, S.; Witte, G.; Wöll, C. Epitaxial Growth of Pentacene Films on Metal Surfaces. *ChemPhysChem* **2004**, *5*, 266−270.
(25) Brondijk, J. J.; Roelofs, W. S. C.; Mathijssen, S. G. J.; Shehu, A.; Cramer, T.; Biscarini, F.; Blom, P. W. M.; de Leeuw, D. M. Two-Dimensional Charge Transport in Disordered Organic Semiconductors. *Phys. Rev. Lett.* **2012**, *109*, 056601.
(26) Kronemeijer, A. J.; Pecunia, V.; Venkateshvaran, D.; Nikolka, M.; Sadhanala, A.; Moriarty, J.; Szumilo, M.; Sirringhaus, H. Two-Dimensional Carrier Distribution in Top-Gate Polymer Field-Effect Transistors: Correlation between Width of Density of Localized States and Urbach Energy. *Adv. Mater.* **2014**, *26*, 728−733.
(27) Vissenberg, M. C. J. M.; Matters, M. Theory of the Field-Effect Mobility in Amorphous Organic Transistors. *Phys. Rev. B* **1998**, *57*, 12964−12967.
(28) Dinelli, F.; Murgia, M.; Levy, P.; Cavallini, M.; Biscarini, F.; de Leeuw, D. M. Spatially Correlated Charge Transport in Organic Thin Film Transistors. *Phys. Rev. Lett.* **2004**, *92*, 116802.
(29) Shehu, A.; Quiroga, S. D.; D'Angelo, P.; Albonetti, C.; Borgatti, F.; Murgia, M.; Scorzoni, A.; Stoliar, P.; Biscarini, F. Layered Distribution of Charge Carriers in Organic Thin Film Transistors. *Phys. Rev. Lett.* **2010**, *104*, 246602.
(30) Ruiz, R.; Papadimitratos, A.; Mayer, A. C.; Malliaras, G. G. Thickness Dependence of Mobility in Pentacene Thin-Film Transistors. *Adv. Mater.* **2005**, *17*, 1795−1798.
(31) Miozzo, L.; Yassar, A.; Horowitz, G. Surface Engineering for High Performance Organic Electronic Devices: The Chemical Approach. *J. Mater. Chem.* **2010**, *20*, 2513.

DOI: 10.1021/am507528e
ACS Appl. Mater. Interfaces 2015, 7, 1833−1840